EJN fens European Journal of Neuroscience

European Journal of Neuroscience, pp. 1–12, 2013 doi:10.1111/ejn.12175

Frames of reference for eye–head gaze shifts evoked during frontal eye field stimulation

Jachin A. Monteon,[1,2,3] Hongying Wang,[1,2] Julio Martinez-Trujillo[4] and J. Douglas Crawford[1,2,3,5]
[1]Centre for Vision Research, York University, Toronto, ON, Canada
[2]Canadian Action and Perception Network, Toronto, ON, Canada
[3]Department of Biology, York University, Toronto, ON, Canada
[4]Department of Physiology, McGill University, Montreal, QC, Canada
[5]Department of Psychology and School of Kinesiology and Health Sciences, York University, Toronto, ON, Canada

Keywords: frontal cortex, frontal eye field, gaze control, monkey, reference frames

Abstract

The frontal eye field (FEF), in the prefrontal cortex, participates in the transformation of visual signals into saccade motor commands and in eye–head gaze control. The FEF is thought to show eye-fixed visual codes in head-restrained monkeys, but it is not known how it transforms these inputs into spatial codes for head-unrestrained gaze commands. Here, we tested if the FEF influences desired gaze commands within a simple eye-fixed frame, like the superior colliculus (SC), or in more complex egocentric frames like the supplementary eye fields (SEFs). We electrically stimulated 95 FEF sites in two head-unrestrained monkeys to evoke 3D eye–head gaze shifts and then mathematically rotated these trajectories into various reference frames. In theory, each stimulation site should specify a specific spatial goal when the evoked gaze shifts are plotted in the appropriate frame. We found that these motor output frames varied site by site, mainly within the eye-to-head frame continuum. Thus, consistent with the intermediate placement of the FEF within the high-level circuits for gaze control, its stimulation-evoked output showed an intermediate trend between the multiple reference frame codes observed in SEF-evoked gaze shifts and the simpler eye-fixed reference frame observed in SC-evoked movements. These results suggest that, although the SC, FEF and SEF carry eye-fixed information at the level of their unit response fields, this information is transformed differently in their output projections to the eye and head controllers.

Introduction

A fundamental question in systems neuroscience is how the brain uses sensory information to plan and perform a movement. For instance, visual information enters the nervous system through photoreceptors that are fixed to the eye but this information must eventually be used to control movements of effectors, such as muscles from the head, torso, arms and eyes. The execution of movement towards a sensory target requires a transformation from the encoded sensory signal into a motor command suitable to drive the muscle. This transformation is a critical component of sensory guided movement processing and has been referred to as a reference frame transformation (Soechting & Flanders, 1992; Colby & Goldberg, 1999; Andersen & Buneo, 2002; Cohen & Andersen, 2002; Crawford *et al.*, 2011; DeSouza *et al.*, 2011).

Numerous studies suggest that gaze control structures such as the lateral intra-parietal cortex (LIP) and the superior colliculus (SC) encode gaze commands in a simple eye-fixed reference frame (Colby *et al.*, 1995; Klier *et al.*, 2001; Andersen & Buneo, 2002; Cohen & Andersen, 2002; Constantin *et al.*, 2009). This has contributed to the conjecture that the early stages of visuomotor processing rely almost exclusively on eye-fixed coordinates, staving off the visuomotor reference frame transformation for later stages of processing (Klier *et al.*, 2001; Martinez-Trujillo *et al.*, 2004). However, this simple description may only pertain to relatively direct transformations from vision to action (Martinez-Trujillo *et al.*, 2004).

Primates are also capable of more complex gaze behaviors, such as gaze shifts to allocentric-defined targets (Olson & Gettner, 1995; Galati *et al.*, 2000; Dean & Platt, 2006), planned sequences of movements (Lu *et al.*, 2002; Isoda & Tanji, 2004) and saccades to non-visual targets like the hand (Groh & Sparks, 1996; Ren *et al.*, 2006). The frontal cortex may be specialized to support these additional computational demands. For example, unit recording studies have shown that supplementary eye field (SEF) neurons can encode visual targets in eye-fixed (Russo & Bruce, 1996) or object-fixed coordinates (Olson & Gettner, 1999).

However, neural activity probed by unit recording does not necessarily match the encoded goal of the stimulation-evoked movements. For instance, saccades evoked by SEF stimulation have been reported to converge toward head-fixed gaze directions (Tehovnik *et al.*, 1998), eye-, head- or body-fixed goals (Schlag & Schlag-Rey,

Correspondence: Dr J. D. Crawford, [5]Department of Psychology and School of Kinesiology and Health Sciences, as above.
E-mail: jdc@yorku.ca

Received 5 October 2010, revised 14 January 2013, accepted 30 January 2013

1987; Martinez-Trujillo *et al.*, 2004), depending on the exact site of stimulation. Such findings have led to the proposal that the frontal cortex provides an alternative stream of visuomotor processing for the transformation of visual information in retinal or object-fixed coordinates into any potential motor frame (Olson & Gettner, 1995; Martinez-Trujillo *et al.*, 2004).

Where do the frontal eye fields (FEFs) fit into this scheme? The FEF is a region of the prefrontal cortex that shows saccade-related signals (Bruce & Goldberg, 1985; Bruce *et al.*, 1985), has reciprocal connections with both the LIP (Petrides & Pandya, 1984; Andersen *et al.*, 1985) and SEF (Huerta & Kaas, 1990; Matelli *et al.*, 1991; Schall *et al.*, 1993; Stanton *et al.*, 1993), and has outputs to both the SC (Komatsu & Suzuki, 1985) and directly to the brainstem reticular formation (Sparks & Hartwich-Young, 1989; Segraves, 1992).

Classically, the FEF has been assumed to use primarily eye-fixed representation of space, because neurons in this area usually encode visual or motor events with respect to the current of the eyes (Dassonville *et al.*, 1992; Russo & Bruce, 1996; Tehovnik *et al.*, 2000; Van Pelt *et al.*, 2010). Neurons in the FEF show eye-fixed visual receptive fields and appear to code saccades as the vector difference between initial and final eye position (Bruce & Goldberg, 1985; Goldberg & Bruce, 1990; Schall, 1991). Furthermore, several electrical stimulation studies have shown that the FEF can evoke fixed-vector saccades (Robinson & Fuchs, 1969; Russo & Bruce, 1993, 1996) that display little or no initial eye position dependency (Russo & Bruce, 1993, 1996). However, when stimulation in the FEF is applied at the onset of voluntary saccades (colliding saccade paradigm), the resulting evoked eye movements compensate for a portion of the change in eye position of the voluntary movement before stimulation, suggesting that these stimulation-evoked goals can be updated by endogenous signals within the brain (Schlag & Schlag-Rey, 1990; Mushiake *et al.*, 1999). At the unit recording level FEF neurons also show more complex modulations related to eye position (Balan & Ferrera, 2003) and even hand position (Thura *et al.*, 2011).

One limitation of many of these early studies is that they were done with the head restrained. Several studies have examined gaze shifts evoked during stimulation of the FEF in head-unrestrained conditions, and most of these concluded that it is involved in the production of gaze shifts that include both eye and head movement (Tu & Keating, 2000; Chen, 2006; Elsley *et al.*, 2007; Knight & Fuchs, 2007; Monteon *et al.*, 2010). However, these studies focused on the issue of whether the FEF encodes eye or eye + head movements, and did not provide the rigorous analysis of initial and final gaze positions required to provide a reference frame analysis. Thus, most of what we know about the reference frame(s) of FEF-evoked eye movements arises from studies examining small saccades in head-restrained monkeys.

There is reason to believe that 'freeing' the head to provide more natural eye + head movements could change both the way gaze shifts are coded and the results of experimental measurements. For example, stimulation-evoked gaze shifts tend to be larger if the head is free to move compared with when the head is fixed (Martinez-Trujillo *et al.*, 2003a; Gandhi & Sparks, 2004). More importantly, the goal of stimulation-evoked saccades can be strongly misrepresented in head-restrained preparations (Pare *et al.*, 1994; Freedman *et al.*, 1996; Martinez-Trujillo *et al.*, 2003a, 2004; Gandhi & Sparks, 2004). Moreover, the distinction between head-fixed and space/body-fixed schemes is undetectable in the head-restrained animal (Martinez-Trujillo *et al.*, 2004). Thus, we chose to examine reference frames in gaze shifts evoked during brain stimulation in the head-unrestrained animal (Klier *et al.*, 2001; Martinez-Trujillo *et al.*, 2004; Constantin *et al.*, 2007).

The basic assumption behind our approach, as in other similar stimulation/reference frame studies (Klier *et al.*, 2001; Martinez-Trujillo *et al.*, 2004; Constantin *et al.*, 2007), is that stimulation-evoked gaze shifts should converge as a function of initial gaze position toward a unique gaze goal, but only if this goal is represented in the appropriate frame of the stimulation site. In order to provide a complete analysis in head-unrestrained conditions, it is important to record three-dimensional (3D) movements and provide a non-linear 3D analysis (Klier *et al.*, 2001; Martinez-Trujillo *et al.*, 2004; Constantin *et al.*, 2007). For the present purposes this is not because we are interested in torsional rotations of the eye during gaze shifts (Klier *et al.*, 2003), but rather to account for non-linear influences of initial eye/head/gaze orientation on the gaze shift. For example, in head-unrestrained gaze fixations, the eye shows much larger torsional variability around the line of sight, which alters retina/eye-fixed directions relative to space coordinates. Moreover, even in the absence of torsion, gaze shifts show non-linear eye position dependences that grow with the amplitude of movement (Tweed & Vilis, 1987; Crawford *et al.*, 2003). For example, the SC was once thought to code gaze shifts using 'fixed-vector' commands (van Opstal *et al.*, 1991) or using spatial goals (Straschill & Rieger, 1973) depending on the region stimulated, but a 3D analysis showed that this is simply the way an eye-fixed representation of desired gaze projects onto space-fixed coordinates (Klier *et al.*, 2001). It is therefore likely that the SC encodes a single functional signal of desired gaze displacement (Galiana & Guitton, 1992; Freedman *et al.*, 1996).

One limitation inherent to cortical stimulation is the altered cooperation/competition between neurons (Cohen *et al.*, 2010) making it possible that non-physiological patterns of activation add noise to the results (Russo & Bruce, 1993; see Discussion). Another limitation on these experimental techniques is one's ability to interpret the results (Crawford *et al.*, 2011). For instance, physiological studies have shown that the spatial codes derived from unit recordings and those derived from stimulation-evoked movements frequently align (Schiller & Stryker, 1972; Bruce *et al.*, 1985; Hanes & Wurtz, 2001), but several theoretical studies have shown that this is only true in restricted cases (Pellionisz & Llinas, 1985; Zipser & Andersen, 1988; Smith & Crawford, 2005; Blohm *et al.*, 2009). For instance, in neural networks trained to transform eye-fixed visual inputs into head- or body-fixed movement commands, simulated unit recording revealed receptive fields tied to the frame of the sensory input, whereas simulated stimulation of the units produced movements toward goals fixed in the frame of the output targets (Smith & Crawford, 2005; Blohm *et al.*, 2009). Moreover, recording stimulation of intermediate network levels with mixed frames can show a variety of coding schemes (Blohm *et al.*, 2009), much like that observed in some experimental conditions. In general, unit recording and stimulation should only match if there is no reference frame transformation occurring. Thus, one cannot assume that stimulation of the FEF should produce gaze shifts toward the same frame as its visual receptive fields, without already assuming its function.

The purpose of the current study was to re-examine the question of gaze coding in the prefrontal cortex by: (i) stimulating the macaque FEF while recording 3D eye and head rotations; and (ii) using a mathematically correct 3D analysis of the evoked gaze shifts. The methodology employed was the same as that used in our previous studies of the SC (Klier *et al.*, 2001; Constantin *et al.*, 2004), SEF (Martinez-Trujillo *et al.*, 2004) and LIP (Constantin *et al.*, 2007).

The dataset of FEF-evoked movements analysed here was essentially identical to that used in our previous paper (Monteon *et al.*, 2010), in which we found that the evoked gaze shifts showed eye–head coordination patterns highly similar to those seen in normal behavior. Thus, we already know the stimulation sites used in this study evoked coordinated eye/head movements closely resembling volitional gaze shifts, and here we focus only on the question of which frame of reference, if any, best describes the goals for the gaze component of the evoked movements.

Materials and methods

Experiments

Two *Macaca mulatta* monkeys were prepared for 3D eye and head movement recordings. Each animal underwent a surgical procedure under general anesthesia, during which we implanted 3D custom-made coils (copper wires) in the right eye, and a stainless-steel head post and a recording chamber (Crist Instruments) embedded on an acrylic cap on the skull. Two additional orthogonal coils were attached to the acrylic cap during experiments in order to measure head position using the same methodologies and analysis used for our eye coil recordings (Tweed *et al.*, 1990; Crawford *et al.*, 1999). A microstimulation chamber (20 mm diameter) was implanted over the right arcuate sulcus (Robinson & Fuchs, 1969) at 22 mm anterior and 18–20 mm lateral in stereotaxic coordinates, a craniotomy of the frontal bone (20 mm diameter) that covered the base of the chamber allowed access to the FEF. The full details of our methodology and experimental set-up are documented in our previous publication (Monteon *et al.*, 2010). All these procedures were in accordance with the Canadian Council on Animal Care guidelines, and were approved by the York University Animal Care Committee.

During the experiments, the animals wore primate jackets that constrained the movements of the torso but allowed them to freely move their heads (for more details, see Monteon *et al.*, 2010). Animals were trained to fixate previously flashed light-emitting diodes (LEDs) using head-free (head-unrestrained) gaze shifts in the dark (except for the LED emission). They sat in front of a hemispherical screen having a radius of 100 cm. LEDs were 0.4 cm in diameter and affixed to the back of the screen at various eccentricities. The distance between the eyes of the animals and the center of the screen was about 90 cm. Thus, the visual angle covered by the central LED was 0.25 °. Eight LEDs in the array were positioned at 20 ° from a central LED, in radial directions of 0 °, 45 °, 90 °, 135 °, 180 °, 225 °, 270 ° and 315 °. The remaining eight LEDs were positioned at 40 ° distance from the central LED in the same radial directions as the previous round of LEDs.

Behavioral task

Each animal was trained to make visually guided gaze shifts to a step change in target position between two sequentially illuminated LEDs. Animals were allowed to select natural patterns of eye–head coordination. LEDs were illuminated pseudo-randomly to reduce the predictability of the size and direction of the target step. LEDs were illuminated during a pseudo-randomized period that lasted between 300 and 500 ms. If the animal acquired the target during this time it was required to maintain gaze position within a spatial window of 5 –8 ° radius during another period between 300 and 500 ms, otherwise the trial was aborted. Animals received water or juice reward after a pseudo-randomized period between 100 and 200 ms after each completed trial.

Microstimulation parameters

Electrophysiology experiments began after a training period of 3 weeks in each monkey. Stimulation was generated by a stimulator and a constant-current stimulus isolation unit (model S88 and PSIU-6; Grass Instruments), and delivered through a tungsten microelectrode (0.8–1.2 mΩ impedance at 1 kHz, FHC). We monitored the current to be delivered to the electrode by examining the output of the isolation unit; this was done by monitoring the wave shape amplitude of the voltage proportional to the current in an oscilloscope (Hung Chang 5504). The electrode was lowered by a low-weight (48 g) hydraulic micro-drive customized for head-unrestrained experiments (Narishige). Stimulation consisted of cathodal pulses delivered at a pulse rate of 300 Hz, with an individual pulse duration of 0.5 ms. Stimulation duration was controlled by our experimental computer and was set to 200 ms.

During each experiment we made penetrations at one or two locations (tracks) with a maximum excursion of the electrode of 10 mm. Initially, the head was restrained while we searched for a site that could evoke saccadic eye movements at low-current thresholds (sites that evoked movements in at least half of the probes with stimulation parameters of: 300 Hz, 200 ms, < 50 μA). After a low-threshold FEF site was identified, we released the animal's head and delivered higher currents (60–100 μA, typically 80 μA). We used this procedure because it is well documented that higher currents facilitate the engagement of combined eye–head movements (Tu & Keating, 2000; Chen, 2006; Knight & Fuchs, 2007; Monteon *et al.*, 2010). Given such low currents, and the timing and metrics of the evoked movements presented in the Results, we are confident that stimulation was delivered to the low-threshold region of the FEF (Bruce *et al.*, 1985).

Stimulation trials

In the case of the stimulation experiments, stimulation trials were intermixed randomly, with behavioral trials at a ratio of about 1 : 3. Each stimulation trial began at a fixated LED position that was randomly varied across trials to elicit different initial gaze and head positions. The animal fixated the target within a spatial window of 5–8 ° radius and during a pseudorandom period between 300 and 500 ms. Then the LED was extinguished, but animals were trained to maintain gaze within the spatial window where the target was presented an additional pseudo-randomized period between 50 and 300 ms, otherwise the trial was aborted. Stimulation train was delivered within this period and the animal was not required to fixate after stimulation onset. No visual stimulus was present during the electrical stimulation trains. In stimulation trials animals received a water or juice reward 100–200 ms after the stimulation offset, independently of gaze position. After recording the evoked trajectories of a given stimulation site we advanced the electrode by 0.5 mm and repeated the process.

Data analysis

Stimulation-evoked movements were included in the analysis if their gaze peak velocity was > 50 °/s, and the latency from stimulation onset to gaze onset was > 10 ms and < 200 ms. The exceptions were the sites that coded for gaze shifts with amplitudes > 70 °; in this case we allowed a latency from stimulation onset to gaze onset of > 10 ms and < 250 ms. The mean recorded latencies for gaze onsets were 71.05 ± 40.86 ms (M1) and 66.25 ± 37.54 ms (M2; see Monteon *et al.*, 2010 for details). Only the first evoked gaze

shift was analysed; individual trials with multistep gaze shifts were excluded from the analysis. We did not include sites that coded multistep gaze shifts in > 50% of the stimulation-evoked trials. Such movements were excluded because it was difficult to establish if they followed normal eye–head coordination kinematics (Monteon *et al.*, 2010) or be certain of the final goal encoded by the site.

Trials included in the above-mentioned procedure were plotted as quaternions as a function of time. Those representing eye positions at the beginning and end of each stimulation-evoked gaze shift were manually selected by an experienced observer. Trials in which the monkey moved the head during the fixation period by 10 º or more were excluded from the analysis. We only quantitatively analysed data from sites from which we evoked at least 10 movements from different initial gaze positions, which were distributed approximately equally in at least three space quadrants. A total of 95 sites (52 in M1 and 43 in M2) met this condition.

We did not systematically stimulate using other parameters, because our previous study suggested that these parameters evoked movements that closely resembled naturally coordinated eye–head gaze shifts. More specifically, we compared the evoked movements vs. the volitional movements (towards visual targets) in their spatiotemporal properties; their velocity–amplitude relationships; their relative contributions of the eyes and head gaze amplitude; and their vestibulo-ocular reflex torsion. In each of these parameters we found a close match between the natural and stimulation-evoked movements (Monteon *et al.*, 2010). Similar results have been reported by other FEF stimulation studies (Elsley *et al.*, 2007; Knight & Fuchs, 2007; but also see Chen, 2006 for differing findings).

Reference frame analysis

This study employed a theoretical/analytical framework developed previously in this lab for very similar studies of the SC (Klier *et al.*, 2001; Constantin *et al.*, 2004), SEF (Martinez-Trujillo *et al.*, 2004) and LIP (Constantin *et al.*, 2007). This framework was illustrated previously with the use of computer simulations (e.g. Martinez-Trujillo *et al.*, 2004) and so will only be described briefly here. The basic premise is that if the motor output of a population of neurons at a particular site in the brain (via the neurons they project to) predominantly encodes a spatial goal in a particular reference frame, then activation of this population should result in a gaze shift toward that goal, in that particular frame. There are two ways to establish this goal. First, one can rotate stimulation-evoked gaze shifts for a particular site into various frames, and then observe which frame provides the tightest cluster of final gaze positions. This provides a direct comparison between our cardinal models (eye model, space/body model and head model). The second way is to plot the convergence of gaze shifts from individual sites as a function of gaze amplitude, and then compare the whole data distribution to the curves predicted by different models (including a 'fixed-vector' model, in which case there is no convergence). This allows for the possibility of results that fall intermediate between different models. Both methods were employed here, as illustrated below (Figs 4 and 5). These methods have been described in detail elsewhere (e.g. Martinez-Trujillo *et al.*, 2004), so only the essential details follow.

From the raw coil signals, we computed quaternions (q) representing the orientation of the eye-in-space (Es) and head-in-space (Hs) with respect to a reference position in which the eyes and the head were pointing straight ahead. This kind of representation when expressed in a right-hand rule coordinate system aligned with the coils has proven to be accurate for measuring 3D eye and head rotations during gaze movements (Tweed *et al.*, 1990). From the eye-in-space (Es) and head-in-space (Hs) quaternions, we computed the eye-in-head (Eh) quaternions (Crawford *et al.*, 1999) by using the formula $q_{Eh} = q_{Hs} \times q_{Es}^{-1}$. All the quaternions (Es, Hs and Eh) were converted into 3D vectors scaled by their angle of rotation (Crawford & Guitton, 1997) as well as into angular velocity vectors (Crawford & Vilis, 1991) for the off-line analysis.

Quaternions representing the Es trajectories were transformed into eye-fixed coordinates (Fig. 2, last column from left to right) by using first the formula $q_{Ec} = q_{Es} \times q_{EsI}^{-1}$ that multiplies the Es quaternions (q_{Es}) by the inverse of the Es quaternion representing the eye-in-space position at the beginning of the movement (q_{EsI}^{-1}). q_{Ec} represents the quaternions in eye-fixed coordinates. In a similar manner, we transformed the Es quaternions into head-fixed coordinates (q_{Hc}) by using the formula $q_{Hc} = q_{Es} \times q_{HsI}^{-1}$, which multiplies the Es quaternions (q_{Es}) by the inverse of the head-in-space quaternion at the beginning of the movements (q_{HsI}^{-1}). The space/body-fixed coordinates' quaternions were simply the Es quaternions, as during our experiments the bodies of the animals were restrained. The quaternions in the different coordinate systems were converted into 3D vectors scaled by their angle of rotation (Crawford *et al.*, 1999).

In order to determine the goodness of fit of our data to each model, we computed the convergence of the movements in each coordinate system by fitting an ellipse to the end-points of the gaze trajectories using the least-squares method. From the parameters of the ellipse, we computed its area using the formula area = $\pi \times A \times B$, where A and B are the major and minor radius of the ellipse, respectively. This area is an estimate of gaze convergence in the different frames. The comparisons among the areas of the ellipses were conducted using a paired Student's t-test.

For the data analysis shown in Fig. 5, we first computed the characteristic vector (CV) for each site through a multiple linear regression procedure relating the stimulation-evoked displacement of gaze trajectories as a function of initial gaze position. The CV of a given site represents the theoretical gaze trajectory that would be evoked by stimulating the site when the animal is looking straight ahead. Once the CV was obtained, we aligned all the trajectories and the CV with the horizontal meridian. For each individual trajectory, we measured its initial position (IP) and final position (FP) along the abscissa and the ordinate, and by subtracting them we obtained the gaze displacement along both axes (FPx − IPx; FPy − IPy). A convergence index for the movements' direction (CId) was computed by determining the slope by means of a simple linear regression relating the initial position (IPy) and the gaze displacement (FPy − IPy) along the ordinate. A CI for the amplitude of the movement (CIa) was computed by determining the slope by means of a simple linear regression relating the initial position (IPx) and the gaze displacement (FPx − IPx) along the abscissa (Russo & Bruce, 1996; Klier *et al.*, 2001; Martinez-Trujillo *et al.*, 2004). The step-by-step computation of these methods is illustrated in Fig. 3.

For the plots shown in Fig. 5A and B, the CIs and CV were computed in space/body-fixed coordinates. For the CIs and CV shown in Fig. 5C and D, the data were first transformed into head-fixed coordinates. The normalized residuals appearing in Fig. 4E and F were computed by first calculating the residuals squared between the CIs of the stimulation-evoked data appearing in Fig. 5A–D and the CIs predicted (CIp) by the different models for each site $(CI - CIp)^2$. Then, we normalized these squared residuals to the variance (V_r) of the corresponding CI distribution [i.e. $(CI - CIp)^2/V_r$]. This latter normalization was conducted in order to make comparable the data plotted in the different reference frames [i.e. space-fixed

(Fig. 5A and B) and head-fixed (Fig. 5C and D)], which had different variances.

Results

Stimulation-evoked gaze shifts: general observations

We measured 3D eye and head rotations produced by delivering electrical currents (of 60–100 μA and 300 Hz during 200 ms) into 95 different sites in the FEF of two macaques, designated as M1 and M2. These exact stimulation parameters have been shown to evoke kinematically normal gaze shifts when micro-stimulating the same FEF in macaques (Monteon *et al.*, 2010).

Figure 1 shows movement trajectories evoked by stimulating a site in the right FEF of animal M2 (Fig. 1A). The lines represent the trajectories, and the open circles represent their landing positions. The stimulation-evoked gaze trajectories (Fig. 1D) were composed of naturally combined movements of the head-in-space (Fig. 1B) and eye-in-head (Fig. 1C), illustrating previous finding that the FEF evokes coordinated eye–head movements closely resembling volitional gaze shifts (Elsley *et al.*, 2007; Knight & Fuchs, 2007; Monteon *et al.*, 2010). Latencies of the evoked movements (from stimulus onset to movement initiation) were as follows (mean in ms ± SD). Gaze latency movement in M1 was 71.05 ± 40.86 ms (median = 61 ms). Head latency for gaze movements was 82.64 ± 42.60 ms (median = 73 ms). In the case of the second animal, gaze latency was 66.25 ± 37.54 ms (median = 56 ms). Head latency was 78.96 ± 38.22 ms (median = 69 ms). Moreover, gaze shifts (Fig. 1D) started from a variety of different initial eye and head positions, as necessary for our reference frame analysis. Henceforth, we focus on the frame of reference for these gaze shifts.

Fitting eye-, head- and body-fixed reference frames

The question is, do the gaze shifts evoked from this stimulation site converge toward some goal? According to our simulations (Martinez-Trujillo *et al.*, 2004), they should when the data are plotted in the appropriate coordinate system for that site. The right column in Fig. 1 plots the stimulation-evoked gaze trajectories in three different coordinate systems in space/body-fixed coordinates (Fig. 1D), head-fixed coordinates (Fig. 1E) and eye-fixed coordinates (Fig. 1F).

Figure 1 shows that this particular example does not follow the overall pattern predicted by the eye- or space/body-fixed models. There is poor convergence of the trajectories at the FPs in space/body-fixed coordinates (Fig. 1D). When they are plotted in eye-fixed coordinates the FPs show a divergent pattern (Fig. 1F). On the other hand, when the trajectories are plotted in head-fixed coordinates (Fig. 1E), there is strong convergence. Remarkably, this particular FEF site appears to select a desired gaze direction that is fixed relative to the head (Fig. 1E), and then drives both the eye (Fig. 1C) and head (Fig. 1B) to this goal: a head-fixed code for gaze. As we shall see, however, this was not the case for all sites.

We repeated the same analysis (mathematical rotations into different coordinate systems; see Materials and methods) for all of our stimulation sites. Figure 2 shows gaze data from three example sites (arranged in the three columns). For easy visualization, we have plotted the data in space/body-fixed coordinates (Fig. 2A–C), head-fixed coordinates (Fig. 2D–F) and eye-fixed coordinates (Fig. 2G–I). The cartoons in the first row illustrate the reference frame models that best fit the data in each column. We chose these three examples because they illustrate the main observations from our initial analysis.

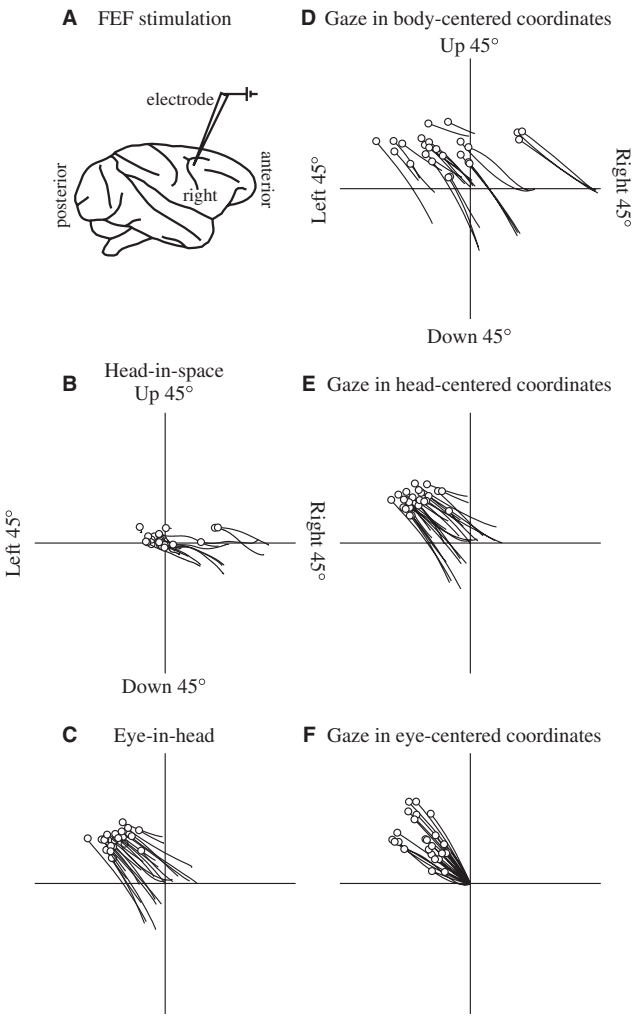

FIG. 1. Example of stimulation-evoked trajectories. (A) Side view of the brain right hemisphere in animal M2; the tip of the electrode indicates the anatomical location of the stimulated site. (B) Behind view of the head-in-space trajectories evoked by stimulating the site. The lines indicate the trajectories, and the small circles indicate their ending position. The abscissa represents the horizontal meridian, and the ordinate represents the vertical meridian. (C) Behind view of the eye-in-head trajectories. The symbols are the same as in (B). (D–F) Gaze trajectories plotted in space/body- (D), head- (E) and eye-fixed coordinates (F). The symbols are the same as in (B) and (C). The axes represent the horizontal (abscissa) and vertical (ordinate) meridians aligned with the center of the reference frame. FEF, frontal eye field.

As we can see, high convergence of the FPs of the trajectories was distributed (although not uniformly) among different coordinate systems depending on the site of stimulation. A few sites had the highest convergence in space/body coordinates (Fig. 2A). At some sites, the data converged best in head-fixed coordinates (Fig. 2E). And for many sites, the evoked gaze shifts converged best when plotted in eye-fixed coordinates (Fig. 2I). These suggest that different FEF sites encode the desired gaze direction in at least three different reference frames. The simplest way to quantify these observations is to focus on only the final gaze directions of the evoked movements, as an indicator of desired gaze direction for that site.

In order to document this for all of our stimulation sites, we fit an ellipse to the cluster of gaze trajectory's end-points in each coordinate system. This is a method of fitting and comparing the models:

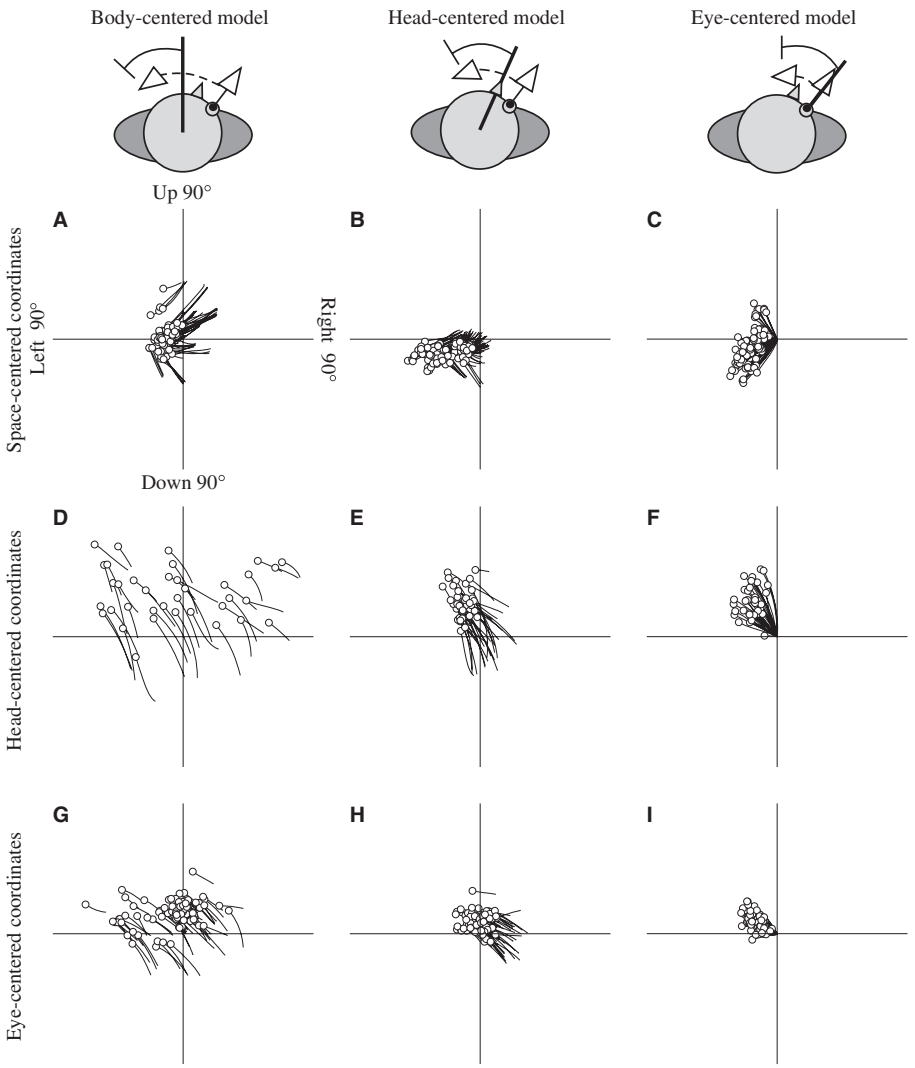

FIG. 2. Stimulation site examples. Gaze trajectories from three different stimulated sites (columns) plotted in space/body (A–C), head (D–F) and eye (G–I) coordinates. The symbols are the same as in Fig. 1. The top row indicates the reference frame in which the trajectories are most likely encoded. Top row: the thick black line represents the pointing direction of the body (left), head (middle) or eye (right). The curved solid line represents the distance to acquire the target relative to the body (left), head (middle) or eye (right). The solid line connected to the white triangle represents gaze (eye-in-space) orientation. The dashed line connected to the white arrow represents the distance to acquire the target relative to current gaze direction.

the coordinate system in which the ellipse is smallest corresponds to the coordinate frame model with the best fit.

Example ellipse fits are shown in the first column of Fig. 4 for one site. The data points represent the end-points of the trajectories plotted in space/body (first row), head (second row) and eye (third row) coordinates. The ellipse with the smallest area is the one corresponding to the head-fixed plot, suggesting that this particular site encodes the desired gaze relative to the pointing direction of the head (roughly orthogonal to the face). We repeated the same procedure for each of the stimulation sites and obtained the ellipses illustrated in the remainder of Fig. 4. The second column shows the actual location of the gaze end-point ellipses for the different sites, whereas the third column realigns them with the center of their coordinate systems for easier visual comparison of the ellipse areas.

Averaged across sites, the eye-fixed ellipse (Fig. 4F) had the smallest area (mean ± SEM; 916.45 ± 146.85 ^{o2}), followed by the head-fixed ellipse (1025.63 ± 105.96 ^{o2}; Fig. 4E) and space/body-fixed ellipse (4063.31 ± 344.90 ^{o2}; Fig. 4D). When comparing the areas of the ellipses among the three reference frames, we found that they were significantly smaller in head- and eye-fixed coordinates than in space/body coordinates ($P < 0.0001$; Student's *t*-test, after Bonferroni correction). However, we did not find statistically significant differences between the areas in head- and eye-fixed coordinates ($P = 0.20$; paired Student's *t*-test).

On a site-by-site basis, the eye frame model provided the best fit in 71% of the stimulation sites, with the head frame and space/body frame providing a better fit in 24 and 5% of the sites, respectively. Even when analysed site by site, the ellipse fits were never perfect in any frame (this would have yielded a single point with zero area). This is not surprising considering the inherent state-dependent neural activity (Gold & Shadlen, 2000) 'downstream' of cortical structures like the FEF (Monteon *et al.*, 2012), which one would expect to randomly affect the results of individual stimulation trials. Thus, an inherent problem in this simple method of model fitting is that it assumes that each FEF site perfectly follows one reference frame model, whereas in reality individual sites might fall within a continuum between these models.

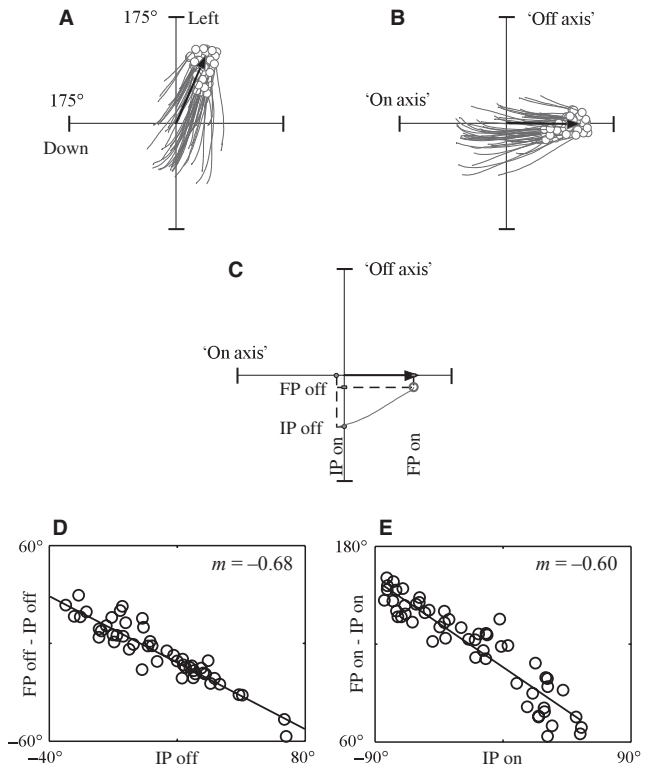

FIG. 3. Step-by-step computation of parameters used to obtain the CI. (A) Gaze trajectories evoked by micro-stimulating one site in the right FEF. The vectors are plotted according to the right-hand rule, and the dark arrow represents the characteristic gaze vector for the particular site (see Materials and methods). (B) All the trajectories and the CV have been rotated and aligned with the positive horizontal axis. The new axes are named 'on axis' and 'off axis' according to their orientation relative to the direction parallel or orthogonal (respectively) to the CV. This rotation was necessary to clearly separate the off/on axis components and to be able to compare sites with different CV. (C) For each individual trajectory, measurements of initial positions (IPs) and final positions (FPs) relative to the 'on axis' and 'off axis' were taken. (D) A position dependency index for the direction of the movements was computed through a linear regression procedure relating the IP in the 'off-axis' and the gaze displacement (FP–IP) along the same axis. The resultant slope (m) of the linear fit is equivalent to the CI (D: off-axis; E: on-axis) for this site. (E) A position dependency index for the amplitude of the movements was computed through a linear regression procedure relating the IP in the 'on-axis' and the gaze displacement (FP–IP) along the same axis. The resultant slope (m) of the linear fit is equivalent to the CI for this site.

To address the above-mentioned factors, we used a second, more complex method of quantification that did not rely solely on the potentially noisy end-points of the gaze shifts and that allows one to visualize a complete continuum of representation. We quantified the convergence of the gaze trajectories as a function of initial gaze position and then plotted this as a function of the characteristic gaze displacement vector amplitude calculated for that site (see 'Data analysis').

We then compared these with the predictions of different models of gaze coding (Fig. 5). Negative CI values correspond to converging movements, positive CI values correspond to diverging movements, and zero corresponds to fixed-vector type of movements that are independent of initial eye position. A similar method was used in previous studies of the SC, SEF and LIP (Klier *et al.*, 2001; Martinez-Trujillo *et al.*, 2004; Constantin *et al.*, 2009).

Figure 5A and B shows a scatterplot analysis similar to that in our previous publications (Klier *et al.*, 2001; Martinez-Trujillo *et al.*, 2004; Constantin *et al.*, 2009). Figure 5A shows CIs (ordinate) for the component of gaze orthogonal to the characteristic gaze vector of each site (as a measure of directional convergence), and Fig. 5B shows the CIs for the amplitude component of the gaze shifts (i.e. parallel to the characteristic gaze displacement vector), all plotted as a function of the characteristic gaze displacement vector amplitude for each site (note that this CV does not show the position-dependent variations in movement amplitude for individual trials). The open circles represent data from one animal, and the filled circles represent the data from the second animal. Note that all of these data were computed in space/body-fixed coordinates.

For the CIs the mean ($\pm$ SD) correlation coefficient (R) for the direction of the movements for all our FEF sites was 0.50 ± 0.27 (range; 0.01–0.98); while the value for the amplitude of the movements was 0.48 ± 0.27 (range; 0.0015–0.96). These values were statistically significant (t-statistic $P \leq 0.05$) in 63 out of 95 sites (66%) for the direction of the movements, and in 62 out of 95 sites (65%) for the amplitude of the movements. Note that when the slopes (CI values) are low (i.e. toward the fixed-vector model), one should expect low correlations because there is no relationship between position and the stimulus-evoked movement.

In these graphs, a 'fixed-vector' model of gaze coding – independent of initial gaze position – predicts zero convergence (a horizontal line running along the abscissa), a space/body-fixed coding predicts complete convergence in space (horizontal line at -1 in the ordinate), and an eye-fixed model predicts a non-linear trend (dashed line) in Fig. 5A, with nearly zero convergence in Fig. 5B (for a more complete description of the eye-fixed model, see Klier *et al.*, 2001). Looking first at Fig. 5A, unlike similarly plotted data from the SC (Klier *et al.*, 2001), these data clearly do not follow the predictions of the eye-fixed model (dashed line). The fit is even worse for the 'fixed-vector model'. Nor do the data consistently follow the predictions of a space/body-fixed model (horizontal line at -1 in the ordinate). Instead, some of these data points fall close to the predictions of the eye-fixed model and a few others fall close to the predictions of the space-fixed model. This was also true for the CI for gaze amplitude (Fig. 5B).

One possibility is that the data fit best the predictions of a head-fixed model. In the plots shown in Fig. 5A and B, the predictions of a head-fixed model cannot be represented by a single line, because they differ depending on the relative contributions of the movement of the eyes and head to gaze. This could be different for different animals, for different recording sites, and during different recording sessions. A large head contribution causes the head model to behave like the eye model, whereas a negligible head contribution causes the head model to become equal to the space/body model. Thus, in this plot one cannot distinguish whether the data are following the head model or falling within a true continuum, as suggested indirectly in our previous analysis (Figs 2 and 4). To address this issue, we performed a different analysis.

We first rotated the gaze trajectories for the different sites in head-fixed coordinates and then recomputed the CIs for the direction and amplitude of the trajectories. This method allowed us to generate a single curve with the predictions of the head-fixed model (horizontal line at -1 in the ordinate of the panels in the second row). In these plots (Fig. 5C and D), the data falling along the CI = -1 line fit better the predictions of the head-fixed model, the data falling far below the line fit better the predictions of the eye-fixed model, and the data falling well above the line fit better the predictions of the space/body-fixed model. The frequency histograms on the right sides of these panels show that the data fall somewhere between the eye model and head model predictions. The data point variations showed

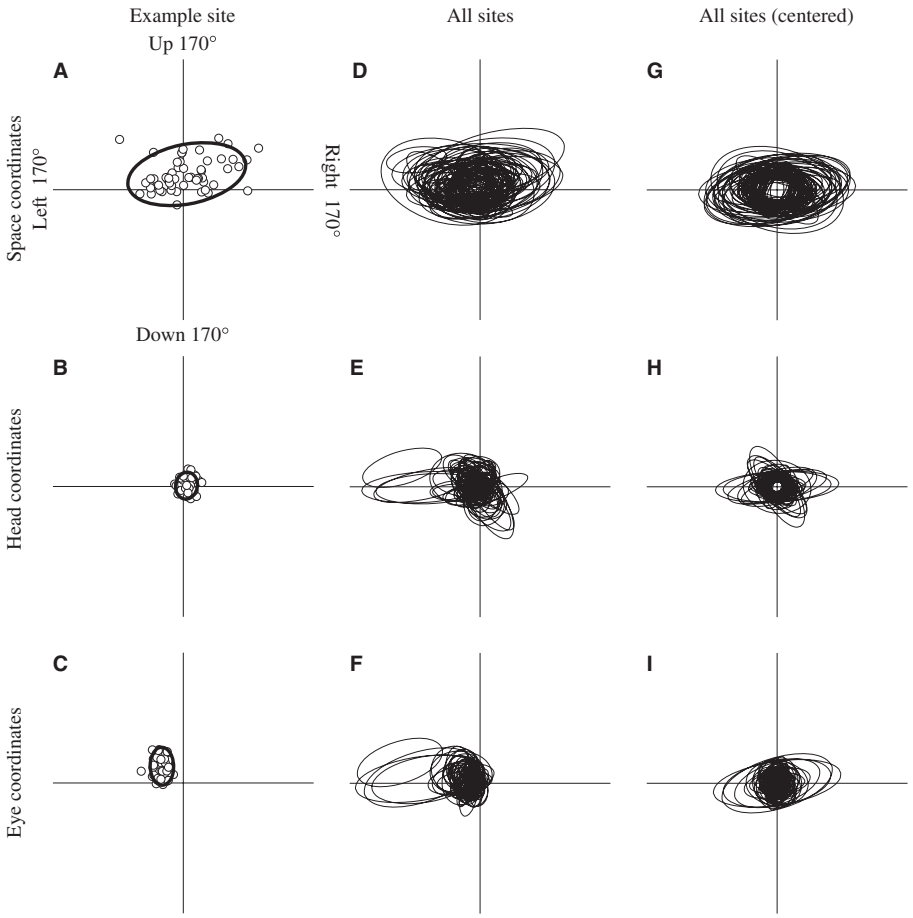

FIG. 4. Gaze convergence in different frames across sites. (A–C) Trajectories' end-points (open circles) and ellipse fitting in space/body (A), head (B) and eye (C) coordinates. The area of the ellipse indicates the convergence of the end-points. (D–F) Ellipses fitted to the end-points of the stimulation-evoked gaze trajectories from the 95 sites in the two animals in space/body- (D), head- (E) and eye-fixed (F) coordinates. (G–I) Same data as in (D–F), but the ellipses have been aligned in such a way that their centers coincide with the centers of the coordinate system.

very little clustering (other than a few sites that produced very large gaze shifts). Instead, they rather scattered in a continuum or gradual transition as they departed from values near the head model predictions.

To further quantify the above observations, we determined the goodness of fit of the data to the different models of gaze coding by computing the squared residuals between the data and the predictions of each model. This method calculates a measure of the discrepancy between the data and the estimation model. A small squared residual indicates a tight fit of the model to the data.

In order to compare the residuals^2 in the head frame (Fig. 5C and D) with those from the other plot (Fig. 5A and B) on an even footing, we first normalized each residual^2 to the variance of the CIs of its corresponding distribution (see 'Data analysis'). The line graphs in Fig. 5E and F show the distribution of the normalized residuals for the CI for the direction component (Fig. 5E) and the amplitude component (Fig. 5F) for the four models.

Considering the population as a whole, we found that for both CIs (direction and amplitude) the mean of the residuals^2 was significantly different across models [one-way analysis of variance (ANOVA), $F = 2.69$; $P < 0.001$; Fig. 5E and F]. A Tukey *post hoc* test revealed that in both the direction and the amplitude components, the eye-fixed and fixed-vector models showed lower residual^2 values than the head- and space-fixed models. There was also a statistical difference between head- and space-fixed models. There was no significant difference between the eye- and fixed-vector models, suggesting that the data were fit equally well by the fixed-vector or the eye-fixed models. Although the test showed no statistical significance, the mean of the normalized residuals for the CI for direction was the lowest for the eye-fixed model (mean $\pm$ SEM; 0.055 ± 0.010), when compared with the fixed-vector model (0.080 ± 0.014). Then the values increased for the head-fixed model (0.270 ± 0.021) and the space-fixed model (0.661 ± 0.027).

We also examined squared residuals curves with the lowest values for all the FEF sites. We found that for the direction CI in space/body coordinates (Fig. 5A) the eye-fixed model produced the lowest residuals in the overwhelming majority of sites (76 sites/80%), followed by the head-fixed model (nine sites/10%), the fixed-vector model (eight sites/8%) and finally the space-fixed model (two sites/2%). This pattern of distribution agrees closely with the general pattern that was observed using the elliptical fit method (Fig. 5). However, using the CI method (Fig. 5A–C) one can clearly see that the full distribution of data is best characterized as a continuum of coding between eye-fixed to head-fixed coding, with a low propensity toward sites in the space coding range.

Discussion

The current study recorded head-unrestrained gaze shifts evoked from a large set of electrically stimulated FEF sites, we analysed

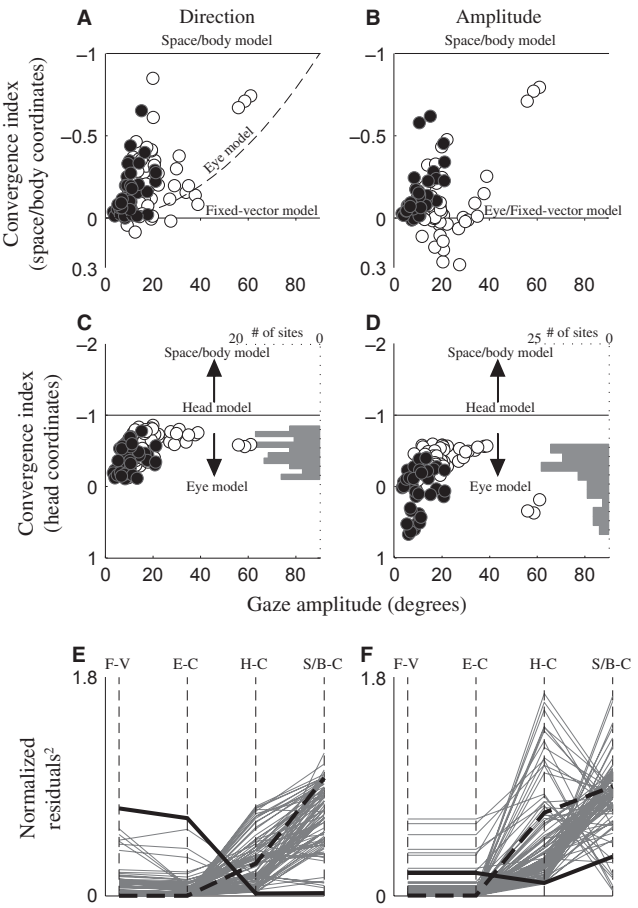

FIG. 5. CIs in different frames. CIs (ordinate) as a function of gaze amplitude (abscissa) for the direction (A and C) and amplitude (B and D) of the stimulation-evoked trajectories in space/body (A and B) and head (C and D) coordinates. Open circles correspond to data from animal M1, and filled circles correspond to data from M2. The right ordinate in (C) and (D) shows the distributions of the CIs. The graphs in the lower row show the residuals² for the fixed-vector (F-V), eye-fixed (E–C), head-fixed (H–C) and space/body-fixed (S/B-C) models for the CI for direction (E) and amplitude (F) of the movements. The thick solid black line shows an example site for which the head-fixed model showed the lowest residuals, and the thick dashed black line shows an example for which the eye-fixed model showed the lowest residuals.

these data in 3D, and compared them with all known models of gaze coding in multiple reference frames. The results of this analysis were consistent with a continuum of coexisting eye- and head-fixed representations for gaze coding in the FEF with a minority of sites possessing a spatial goal. Our results are in agreement with theoretical studies that predict that stimulation of centers involved in visuomotor transformations that possess visual receptive fields could output motor commands in coordinates fixed relative to the head (Zipser & Andersen, 1988; Smith & Crawford, 2005), space or other reference frames (Blohm *et al.*, 2009). To see the full anatomical map of our stimulation sites and the details of the evoked outputs please refer to our previous publication (Monteon *et al.*, 2010).

Previous studies have reported coding of saccadic eye movements in eye-fixed reference frames in the FEF (Dassonville *et al.*, 1992; Russo & Bruce, 1996; Tehovnik *et al.*, 2000). Our results support these previous findings at the majority of our sites (> 70%). However, we also found many of our tested sites coded gaze commands relative to head-fixed coordinates, and sporadically some sites in space-fixed coordinates. As suggested previously, head-fixed stimulation is not a reliable measure of motor output in brain sites that code eye–head gaze (Martinez-Trujillo *et al.*, 2003a, 2004; Gandhi & Sparks, 2004), and indeed freeing the body might further improve such data.

Although it may seem odd at first that the FEF has individual clusters of neural cells driving motor commands in different coordinate systems, it is well known that the FEF has a topographic map for evoked eye movements (Bruce *et al.*, 1985; Fukushima *et al.*, 2000; Chen, 2006; Knight & Fuchs, 2007), as well as topographically organized reciprocal projections with the SC (Sommer & Wurtz, 2000; Hanes & Wurtz, 2001; Crapse & Sommer, 2009) and projections to premotor brainstem structures (King *et al.*, 1980; Sparks & Hartwich-Young, 1989; Segraves, 1992). Thus, it is plausible that neighboring cells share similar coding schemas.

More importantly, our results are in close agreement with literature using the same methodology in other brain centers. For instance, the SC exhibits evoked movements clearly explained by an eye-fixed representation (Klier *et al.*, 2001), here we found about 70% of the FEF sites to be eye-fixed. On the other hand, evoked movements from SEF sites were found to have goals in eye-fixed coordinates, but also in head-fixed and space-fixed coordinates (Martinez-Trujillo *et al.*, 2004), as in the case of the remaining 30% of our FEF sites. Accordingly, our results suggest that the FEF seems to provide an intermediate step between the SEF and the SC in the processing of gaze command signals (Fig. 6). That is, the use of more complex coding (eye, head, body/space frames) may be used in higher cortical areas like the SEF; whereas in the SC a simple eye-based representation is used. This eye-fixed code may be useful for the decomposition of gaze signals into independent eye and head signals necessary in downstream structures.

It is important to note that these coding schemes are not intrinsic to the FEF sites in isolation, but rather are the product of the total pattern of output connectivity activated when these sites were stimulated. Thus, the transformation from activity in the FEF to behavior depends on this full set of output targets and all of their downstream transformations, traced all the way to patterns of muscular activity. This would include projection to areas such as the SC (Komatsu & Suzuki, 1985; Sommer & Wurtz, 2000; Hanes & Wurtz, 2001). For instance, it is possible that the output goals shown in our FEF stimulations are implemented in the SC by modulation of position input signals, we have recently found such modulations in the SC (DeSouza *et al.*, 2011).

One of the assumptions of our study, based on our previous paper (Monteon *et al.*, 2010), is that the areas we stimulated are primarily involved in the coding of gaze direction. As pointed out previously, one alternative interpretation may be that large current spread recruits a larger population of neurons, suggesting that the head motor commands encoded in the FEF may be distributed widely across neuronal populations (Chen, 2006). It is also possible that internal states of motor or cognitive sets (Wise & Kurata, 1989; Miller & Cohen, 2001; Monteon *et al.*, 2012) have an influence on the sensitivity to recruit head movements, but this possibility needs to be explored in future studies. Until this is established, we maintain that the simplest explanation for our results is that the FEF is primarily involved in the coding of gaze (Monteon *et al.*, 2010).

Our results do not necessarily suggest that natural patterns of muscular activity were caused by FEF stimulation (Elsley *et al.*, 2007). In fact, electrical stimulation fails to activate neural elements as when a natural discharge occurs and may fail to engage important neural regions like the cerebellum (Ranck, 1975; Russo & Bruce,

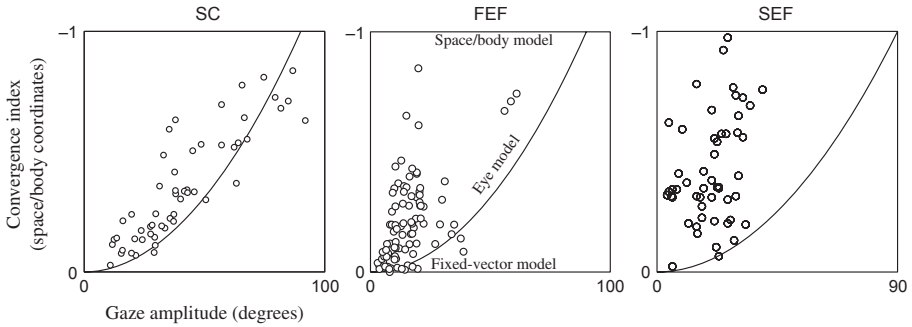

FIG. 6. CIs across gaze centers. Different frames CIs (ordinate) as a function of gaze amplitude (abscissa) for the direction in space/body coordinates. Circles correspond to data from sites in three different brain areas: the superior colliculus (SC, left); the frontal eye field (FEF, middle); and the supplementary eye field (SEF, right). SC data (left panel) were adapted with permission from Klier *et al.* (2001), Macmillan Publishers Ltd, copyright (2001). SEF data (right panel) were modified with permission from Martinez-Trujillo *et al.* (2004).

1993; Tehovnik, 1996; Tehovnik & Slocum, 2000; Tehovnik *et al.*, 2006; Elsley *et al.*, 2007; Histed *et al.*, 2009), and engages both orthodromic and antidromic activation, although the effects in the former are thought to be more robust (Watson *et al.*, 1982; Yeomans, 1990). Similarly, different stimulation parameters might significantly alter the evoked movement's kinematics and potentially their goal (reference frame) as well. For instance, longer stimulation train durations in the FEF have shown to cause an increase in gaze and head movement's amplitude (Knight & Fuchs, 2007). For the current study we analysed 200-ms train durations because our team and others have found stimulation trains of about 200 ms to provide the best emulation of natural head-free gaze shifts from the FEF and other high-level gaze centers (Tu & Keating, 2000; Martinez-Trujillo *et al.*, 2003b; Knight & Fuchs, 2007; Monteon *et al.*, 2010). Even after considering the limitations of this technique, if stimulation reveals a particular frame of reference for a movement goal, this at least provides an 'existence proof' that such a pattern of activation at the site is able to code this goal, even if it is not used this way during normal physiological activity. Nonetheless, except for the exact activation patterns of neck muscles and some kinematic particulars, numerous previous findings show that FEF stimulation can produce gaze command composed of eye–head coordinated movements that closely resemble behavioral gaze shifts (Elsley *et al.*, 2007; Knight & Fuchs, 2007; Monteon *et al.*, 2010). These add credence to our assumption that the coding schemes revealed in our experiment reveal aspects of normal physiology.

There have been exceptions where stimulation of the FEF or surrounding region produced isolated head movements (Chen, 2006) or abnormal torsional head movements (Monteon *et al.*, 2010), but this was never the case in the dataset analysed here. Moreover, if gross electrical input to the FEF can evoke gaze shifts in multiple frames of reference, it seems difficult to argue that more subtle and varied patterns of physiological input could not reproduce similar patterns of motor output. Nevertheless, the main finding we observed from our data is that activation within the FEF can produce gaze shifts toward the goals and reference frames we described, without necessarily knowing if these particular patterns are ever used physiologically.

Implications for the gaze control system

Assuming, for the moment, that the results from the current study are correctly analysed and interpreted, how do they compare with previous studies? About 70% of our sites appeared to use an eye-fixed code or something close to it. This is consistent with the general literature of gaze coding in the SC, LIP and FEF, which appear to employ merely an eye-fixed code to control gaze. (Colby *et al.*, 1995; Russo & Bruce, 1996; Tehovnik *et al.*, 2000; Klier *et al.*, 2001; Andersen & Buneo, 2002; Cohen & Andersen, 2002; Van Pelt *et al.*, 2010). This could reflect a relatively simple transfer of spatial information from the retina to the oculomotor system. It does not seem likely that the FEF is required to produce eye-to-head or eye-to-space reference frame transformations for simple visuomotor transformations, because the lower level SC appears to use an eye-fixed code for eye/head gaze shifts (Klier *et al.*, 2001). It thus appears that the brainstem itself can transform eye-fixed signals into muscle coordinates without the FEF.

However, this does not account for the ~30% of sites in our study that did not show an eye-centered code. How can we account for these? First, there is no reason to assume that the FEF must use the same code as the SC and LIP (indeed, it looks something more like SEF in that respect). Second, our study was done in natural head-unrestrained conditions with only minimal amounts of training, i.e. for the monkey to briefly fixate a light before stimulation. Most previous studies were done in head-restrained conditions in monkeys that were over-trained to produce visually guided saccades. Task experience/training is known to influence neural patterns (Moorman & Olson, 2007; Campos *et al.*, 2010) and the results of stimulation (Gold & Shadlen, 2000; Barborica & Ferrera, 2004; Monteon *et al.*, Submitted). It is possible that these non-retinal sites are involved in different, more complex behaviors. For example, there is some suggestion that the FEF might be involved in aspects of eye–hand coordination (Ren *et al.*, 2008; Thura *et al.*, 2008) that require head- and body-centered transformations (Scherberger *et al.*, 2003; Ren & Crawford, 2009).

Based on these factors and other findings (Schiller *et al.*, 1987; Olson & Gettner, 1999), we again suggest two separate streams in the visuomotor transformations for gaze control – one for direct, visually guided action, going through the parietal lobe and then through the SC, where the visuomotor reference frame transformation would only occur in the brainstem (Martinez-Trujillo *et al.*, 2004). The second stream performs more complex visuospatial and cognitive tasks (involving top-down attention and target selection in arbitrary visual reference frames), and proceeds from the parietal lobe through the SEF and from there to the FEF and other cognitive and motor systems. Our findings support the view that the FEF might play an important role in the second stream by conveying information from the SEF to the SC (Huerta *et al.*, 1986; Everling & Munoz, 2000). An important question to answer in further studies is how the use of these different streams and reference frames is influenced by specific task demands.

Acknowledgements

This work was supported by the Canadian Institutes of Health Research. J.D.C. holds a Canada Research Chair. J.A.M. received support from CONACYT.

Abbreviations

CI, convergence index; CV, characteristic vector; FEF, frontal eye field; FP, final position; IP, initial position; LED, light-emitting diode; LIP, lateral intra-parietal cortex; SC, superior colliculus; SEF, supplementary eye field.

References

Andersen, R.A. & Buneo, C.A. (2002) Intentional maps in posterior parietal cortex. *Annu. Rev. Neurosci.*, **25**, 189–220.

Andersen, R.A., Asanuma, C. & Cowan, W.M. (1985) Callosal and prefrontal associational projecting cell populations in area 7A of the macaque monkey: a study using retrogradely transported fluorescent dyes. *J. Comp. Neurol.*, **232**, 443–455.

Balan, P.F. & Ferrera, V.P. (2003) Effects of gaze shifts on maintenance of spatial memory in macaque frontal eye field. *J. Neurosci.*, **23**, 5446–5454.

Barborica, A. & Ferrera, V.P. (2004) Modification of saccades evoked by stimulation of frontal eye field during invisible target tracking. *J. Neurosci.*, **24**, 3260–3267.

Blohm, G., Keith, G.P. & Crawford, J.D. (2009) Decoding the cortical transformations for visually guided reaching in 3D space. *Cereb. Cortex*, **19**, 1372–1393.

Bruce, C.J. & Goldberg, M.E. (1985) Primate frontal eye fields. I. Single neurons discharging before saccades. *J. Neurophysiol.*, **53**, 603–635.

Bruce, C.J., Goldberg, M.E., Bushnell, M.C. & Stanton, G.B. (1985) Primate frontal eye fields. II. Physiological and anatomical correlates of electrically evoked eye movements. *J. Neurophysiol.*, **54**, 714–734.

Campos, M., Breznen, B. & Andersen, R.A. (2010) A neural representation of sequential states within an instructed task. *J. Neurophysiol.*, **104**, 2831–2849.

Chen, L.L. (2006) Head movements evoked by electrical stimulation in the frontal eye field of the monkey: evidence for independent eye and head control. *J. Neurophysiol.*, **95**, 3528–3542.

Cohen, Y.E. & Andersen, R.A. (2002) A common reference frame for movement plans in the posterior parietal cortex. *Nat. Rev. Neurosci.*, **3**, 553–562.

Cohen, J.Y., Crowder, E.A., Heitz, R.P., Subraveti, C.R., Thompson, K.G., Woodman, G.F. & Schall, J.D. (2010) Cooperation and competition among frontal eye field neurons during visual target selection. *J. Neurosci.*, **30**, 3227–3238.

Colby, C.L. & Goldberg, M.E. (1999) Space and attention in parietal cortex. *Annu. Rev. Neurosci.*, **22**, 319–349.

Colby, C.L., Duhamel, J.R. & Goldberg, M.E. (1995) Oculocentric spatial representation in parietal cortex. *Cereb. Cortex*, **5**, 470–481.

Constantin, A.G., Wang, H. & Crawford, J.D. (2004) Role of superior colliculus in adaptive eye-head coordination during gaze shifts. *J. Neurophysiol.*, **92**, 2168–2184.

Constantin, A.G., Wang, H., Martinez-Trujillo, J.C. & Crawford, J.D. (2007) Frames of reference for gaze saccades evoked during stimulation of lateral intraparietal cortex. *J. Neurophysiol.*, **98**, 696–709.

Constantin, A.G., Wang, H., Monteon, J.A., Martinez-Trujillo, J.C. & Crawford, J.D. (2009) 3-Dimensional eye-head coordination in gaze shifts evoked during stimulation of the lateral intraparietal cortex. *Neuroscience*, **164**, 1284–1302.

Crapse, T.B. & Sommer, M.A. (2009) Frontal eye field neurons with spatial representations predicted by their subcortical input. *J. Neurosci.*, **29**, 5308–5318.

Crawford, J.D. & Guitton, D. (1997) Visual-motor transformations required for accurate and kinematically correct saccades. *J. Neurophysiol.*, **78**, 1447–1467.

Crawford, J.D. & Vilis, T. (1991) Axes of eye rotation and Listing's law during rotations of the head. *J. Neurophysiol.*, **65**, 407–423.

Crawford, J.D., Ceylan, M.Z., Klier, E.M. & Guitton, D. (1999) Three-dimensional eye-head coordination during gaze saccades in the primate. *J. Neurophysiol.*, **81**, 1760–1782.

Crawford, J.D., Martinez-Trujillo, J.C. & Klier, E.M. (2003) Neural control of three-dimensional eye and head movements. *Curr. Opin. Neurobiol.*, **13**, 655–662.

Crawford, J.D., Henriques, D.Y. & Medendorp, W.P. (2011) Three-dimensional transformations for goal-directed action. *Annu. Rev. Neurosci.*, **34**, 309–331.

Dassonville, P., Schlag, J. & Schlag-Rey, M. (1992) The frontal eye field provides the goal of saccadic eye movement. *Exp. Brain Res.*, **89**, 300–310.

Dean, H.L. & Platt, M.L. (2006) Allocentric spatial referencing of neuronal activity in macaque posterior cingulate cortex. *J. Neurosci.*, **26**, 1117–1127.

DeSouza, J.F., Keith, G.P., Yan, X., Blohm, G., Wang, H. & Crawford, J.D. (2011) Intrinsic reference frames of superior colliculus visuomotor receptive fields during head-unrestrained gaze shifts. *J. Neurosci.*, **31**, 18313–18326.

Elsley, J.K., Nagy, B., Cushing, S.L. & Corneil, B.D. (2007) Widespread presaccadic recruitment of neck muscles by stimulation of the primate frontal eye fields. *J. Neurophysiol.*, **98**, 1333–1354.

Everling, S. & Munoz, D.P. (2000) Neuronal correlates for preparatory set associated with pro-saccades and anti-saccades in the primate frontal eye field. *J. Neurosci.*, **20**, 387–400.

Freedman, E.G., Stanford, T.R. & Sparks, D.L. (1996) Combined eye-head gaze shifts produced by electrical stimulation of the superior colliculus in rhesus monkeys. *J. Neurophysiol.*, **76**, 927–952.

Fukushima, K., Sato, T., Fukushima, J., Shinmei, Y. & Kaneko, C.R. (2000) Activity of smooth pursuit-related neurons in the monkey periarcuate cortex during pursuit and passive whole-body rotation. *J. Neurophysiol.*, **83**, 563–587.

Galati, G., Lobel, E., Vallar, G., Berthoz, A., Pizzamiglio, L. & Le Bihan, D. (2000) The neural basis of egocentric and allocentric coding of space in humans: a functional magnetic resonance study. *Exp. Brain Res.*, **133**, 156–164.

Galiana, H.L. & Guitton, D. (1992) Central organization and modeling of eye-head coordination during orienting gaze shifts. *Ann. NY Acad. Sci.*, **656**, 452–471.

Gandhi, N.J. & Sparks, D.L. (2004) *Changing Views of the Role of Superior Colliculus in the Control of Gaze the Visual Neurosciences*. MIT Press, Cambridge, Mass., pp. 2 v. (various pagings).

Gold, J.I. & Shadlen, M.N. (2000) Representation of a perceptual decision in developing oculomotor commands. *Nature*, **404**, 390–394.

Goldberg, M.E. & Bruce, C.J. (1990) Primate frontal eye fields. III. Maintenance of a spatially accurate saccade signal. *J. Neurophysiol.*, **64**, 489–508.

Groh, J.M. & Sparks, D.L. (1996) Saccades to somatosensory targets I. behavioral characteristics. *J. Neurophysiol.*, **75**, 412–427.

Hanes, D.P. & Wurtz, R.H. (2001) Interaction of the frontal eye field and superior colliculus for saccade generation. *J. Neurophysiol.*, **85**, 804–815.

Histed, M.H., Bonin, V. & Reid, R.C. (2009) Direct activation of sparse, distributed populations of cortical neurons by electrical microstimulation. *Neuron*, **63**, 508–522.

Huerta, M.F. & Kaas, J.H. (1990) Supplementary eye field as defined by intracortical microstimulation: connections in macaques. *J. Comp. Neurol.*, **293**, 299–330.

Huerta, M.F., Krubitzer, L.A. & Kaas, J.H. (1986) Frontal eye field as defined by intracortical microstimulation in squirrel monkeys, owl monkeys, and macaque monkeys: I. Subcortical connections. *J. Comp. Neurol.*, **253**, 415–439.

Isoda, M. & Tanji, J. (2004) Participation of the primate presupplementary motor area in sequencing multiple saccades. *J. Neurophysiol.*, **92**, 653–659.

King, W.M., Precht, W. & Dieringer, N. (1980) Synaptic organization of frontal eye field and vestibular afferents to interstitial nucleus of Cajal in the cat. *J. Neurophysiol.*, **43**, 912–928.

Klier, E.M., Wang, H. & Crawford, J.D. (2001) The superior colliculus encodes gaze commands in retinal coordinates. *Nat. Neurosci.*, **4**, 627–632.

Klier, E.M., Martinez-Trujillo, J.C., Medendorp, W.P., Smith, M.A. & Crawford, J.D. (2003) Neural control of 3-D gaze shifts in the primate. *Prog. Brain Res.*, **142**, 109–124.

Knight, T.A. & Fuchs, A.F. (2007) Contribution of the frontal eye field to gaze shifts in the head-unrestrained monkey: effects of microstimulation. *J. Neurophysiol.*, **97**, 618–634.

Komatsu, H. & Suzuki, H. (1985) Projections from the functional subdivisions of the frontal eye field to the superior colliculus in the monkey. *Brain Res.*, **327**, 324–327.

Lu, X., Matsuzawa, M. & Hikosaka, O. (2002) A neural correlate of oculomotor sequences in supplementary eye field. *Neuron*, **34**, 317–325.

Martinez-Trujillo, J.C., Klier, E.M., Wang, H. & Crawford, J.D. (2003a) Contribution of head movement to gaze command coding in monkey frontal cortex and superior colliculus. *J. Neurophysiol.*, **90**, 2770–2776.

Martinez-Trujillo, J.C., Wang, H. & Crawford, J.D. (2003b) Electrical stimulation of the supplementary eye fields in the head-free macaque evokes kinematically normal gaze shifts. *J. Neurophysiol.*, **89**, 2961–2974.

Martinez-Trujillo, J.C., Medendorp, W.P., Wang, H. & Crawford, J.D. (2004) Frames of reference for eye-head gaze commands in primate supplementary eye fields. *Neuron*, **44**, 1057–1066.

Matelli, M., Luppino, G. & Rizzolatti, G. (1991) Architecture of superior and mesial area 6 and the adjacent cingulate cortex in the macaque monkey. *J. Comp. Neurol.*, **311**, 445–462.

Miller, E.K. & Cohen, J.D. (2001) An integrative theory of prefrontal cortex function. *Annu. Rev. Neurosci.*, **24**, 167–202.

Monteon, J.A., Constantin, A.G., Wang, H., Martinez-Trujillo, J. & Crawford, J.D. (2010) Electrical stimulation of the frontal eye fields in the head-free macaque evokes kinematically normal 3D gaze shifts. *J. Neurophysiol.*, **104**, 3462–3475.

Monteon, J.A., Avillac, M., Wang, H., Yan, X. & Crawford, J.D. (2012) Cue-dependent eye-head coordination strategies during stimulation of the frontal eye field. *J. Neurophysiol.*, **108**, 2689–2707.

Moorman, D.E. & Olson, C.R. (2007) Impact of experience on the representation of object-centered space in the macaque supplementary eye field. *J. Neurophysiol.*, **97**, 2159–2173.

Mushiake, H., Fujii, N. & Tanji, J. (1999) Microstimulation of the lateral wall of the intraparietal sulcus compared with the frontal eye field during oculomotor tasks. *J. Neurophysiol.*, **81**, 1443–1448.

Olson, C.R. & Gettner, S.N. (1995) Object-centered direction selectivity in the macaque supplementary eye field. *Science*, **269**, 985–988.

Olson, C.R. & Gettner, S.N. (1999) Macaque SEF neurons encode object-centered directions of eye movements regardless of the visual attributes of instructional cues. *J. Neurophysiol.*, **81**, 2340–2346.

van Opstal, A.J., Hepp, K., Hess, B.J., Straumann, D. & Henn, V. (1991) Two- rather than three-dimensional representation of saccades in monkey superior colliculus. *Science*, **252**, 1313–1315.

Pare, M., Crommelinck, M. & Guitton, D. (1994) Gaze shifts evoked by stimulation of the superior colliculus in the head-free cat conform to the motor map but also depend on stimulus strength and fixation activity. *Exp. Brain Res.*, **101**, 123–139.

Pellionisz, A. & Llinas, R. (1985) Tensor network theory of the metaorganization of functional geometries in the central nervous system. *Neuroscience*, **16**, 245–273.

Petrides, M. & Pandya, D.N. (1984) Projections to the frontal cortex from the posterior parietal region in the rhesus monkey. *J. Comp. Neurol.*, **228**, 105–116.

Ranck, J.B. Jr. (1975) Which elements are excited in electrical stimulation of mammalian central nervous system: a review. *Brain Res.*, **98**, 417–440.

Ren, L. & Crawford, J.D. (2009) Coordinate transformations for hand-guided saccades. *Exp. Brain Res.*, **195**, 455–465.

Ren, L., Khan, A.Z., Blohm, G., Henriques, D.Y., Sergio, L.E. & Crawford, J.D. (2006) Proprioceptive guidance of saccades in eye-hand coordination. *J. Neurophysiol.*, **96**, 1464–1477.

Ren, L., Cressman, E., Blohm, G., Cheyne, D. & Crawford, J.D. (2008) *Cortical Activation during Visual Memory-Guided And Hand-Guided Saccades: An MEG Study Society For Neuroscience Annual Meeting*. Society for Neuroscience, Washington, DC.

Robinson, D.A. & Fuchs, A.F. (1969) Eye movements evoked by stimulation of frontal eye fields. *J. Neurophysiol.*, **32**, 637–648.

Russo, G.S. & Bruce, C.J. (1993) Effect of eye position within the orbit on electrically elicited saccadic eye movements: a comparison of the macaque monkey's frontal and supplementary eye fields. *J. Neurophysiol.*, **69**, 800–818.

Russo, G.S. & Bruce, C.J. (1996) Neurons in the supplementary eye field of rhesus monkeys code visual targets and saccadic eye movements in an oculocentric coordinate system. *J. Neurophysiol.*, **76**, 825–848.

Schall, J.D. (1991) Neuronal activity related to visually guided saccades in the frontal eye fields of rhesus monkeys: comparison with supplementary eye fields. *J. Neurophysiol.*, **66**, 559–579.

Schall, J.D., Morel, A. & Kaas, J.H. (1993) Topography of supplementary eye field afferents to frontal eye field in macaque: implications for mapping between saccade coordinate systems. *Visual Neurosci.*, **10**, 385–393.

Scherberger, H., Goodale, M.A. & Andersen, R.A. (2003) Target selection for reaching and saccades share a similar behavioral reference frame in the macaque. *J. Neurophysiol.*, **89**, 1456–1466.

Schiller, P.H. & Stryker, M. (1972) Single-unit recording and stimulation in superior colliculus of the alert rhesus monkey. *J. Neurophysiol.*, **35**, 915–924.

Schiller, P.H., Sandell, J.H. & Maunsell, J.H. (1987) The effect of frontal eye field and superior colliculus lesions on saccadic latencies in the rhesus monkey. *J. Neurophysiol.*, **57**, 1033–1049.

Schlag, J. & Schlag-Rey, M. (1987) Evidence for a supplementary eye field. *J. Neurophysiol.*, **57**, 179–200.

Schlag, J. & Schlag-Rey, M. (1990) Colliding saccades may reveal the secret of their marching orders. *Trends Neurosci.*, **13**, 410–415.

Segraves, M.A. (1992) Activity of monkey frontal eye field neurons projecting to oculomotor regions of the pons. *J. Neurophysiol.*, **68**, 1967–1985.

Smith, M.A. & Crawford, J.D. (2005) Distributed population mechanism for the 3-D oculomotor reference frame transformation. *J. Neurophysiol.*, **93**, 1742–1761.

Soechting, J.F. & Flanders, M. (1992) Moving in three-dimensional space: frames of reference, vectors, and coordinate systems. *Annu. Rev. Neurosci.*, **15**, 167–191.

Sommer, M.A. & Wurtz, R.H. (2000) Composition and topographic organization of signals sent from the frontal eye field to the superior colliculus. *J. Neurophysiol.*, **83**, 1979–2001.

Sparks, D.L. & Hartwich-Young, R. (1989) The deep layers of the superior colliculus. *Rev. Oculomot. Res.*, **3**, 213–255.

Stanton, G.B., Bruce, C.J. & Goldberg, M.E. (1993) Topography of projections to the frontal lobe from the macaque frontal eye fields. *J. Comp. Neurol.*, **330**, 286–301.

Straschill, M. & Rieger, P. (1973) Eye movements evoked by focal stimulation of the cat's superior colliculus. *Brain Res.*, **59**, 211–227.

Tehovnik, E.J. (1996) Electrical stimulation of neural tissue to evoke behavioral responses. *J. Neurosci. Meth.*, **65**, 1–17.

Tehovnik, E.J. & Slocum, W.M. (2000) Effects of training on saccadic eye movements elicited electrically from the frontal cortex of monkeys. *Brain Res.*, **877**, 101–106.

Tehovnik, E.J., Slocum, W.M., Tolias, A.S. & Schiller, P.H. (1998) Saccades induced electrically from the dorsomedial frontal cortex: evidence for a head-centered representation. *Brain Res.*, **795**, 287–291.

Tehovnik, E.J., Sommer, M.A., Chou, I.H., Slocum, W.M. & Schiller, P.H. (2000) Eye fields in the frontal lobes of primates. *Brain Res. Brain Res. Rev.*, **32**, 413–448.

Tehovnik, E.J., Tolias, A.S., Sultan, F., Slocum, W.M. & Logothetis, N.K. (2006) Direct and indirect activation of cortical neurons by electrical micrstimulation. *J. Neurophysiol.*, **96**, 512–521.

Thura, D., Hadj-Bouziane, F., Meunier, M. & Boussaoud, D. (2008) Hand position modulates saccadic activity in the frontal eye field. *Behav. Brain Res.*, **186**, 148–153.

Thura, D., Hadj-Bouziane, F., Meunier, M. & Boussaoud, D. (2011) Hand modulation of visual, preparatory, and saccadic activity in the monkey frontal eye field. *Cereb. Cortex*, **21**, 853–864.

Tu, T.A. & Keating, E.G. (2000) Electrical stimulation of the frontal eye field in a monkey produces combined eye and head movements. *J. Neurophysiol.*, **84**, 1103–1106.

Tweed, D. & Vilis, T. (1987) Implications of rotational kinematics for the oculomotor system in three dimensions. *J. Neurophysiol.*, **58**, 832–849.

Tweed, D., Cadera, W. & Vilis, T. (1990) Computing three-dimensional eye position quaternions and eye velocity from search coil signals. *Vision Res.*, **30**, 97–110.

Van Pelt, S., Toni, I., Diedrichsen, J. & Medendorp, W.P. (2010) Repetition suppression dissociates spatial frames of reference in human saccade generation. *J. Neurophysiol.*, **104**, 1239–1248.

Watson, R.E. Jr., Troiano, R., Poulakos, J., Weiner, S. & Siegel, A. (1982) A 14C–2-deoxyglucose analysis of the neural pathways of the limbic forebrain in the rat: II. The hypothalamus. *Brain Res. Bull.*, **8**, 459–476.

Wise, S.P. & Kurata, K. (1989) Set-related activity in the premotor cortex of rhesus monkeys: effect of triggering cues and relatively long delay intervals. *Somatosens. Mot. Res.*, **6**, 455–476.

Yeomans, J.S. (1990) *Principles of Brain Stimulation*. Oxford University Press, New York.

Zipser, D. & Andersen, R.A. (1988) A back-propagation programmed network that simulates response properties of a subset of posterior parietal neurons. *Nature*, **331**, 679–684.